7 September 2026

Molecular Engineering of a Small-Molecular Yellow-to-Orange Carbonyl-based Multi-Resonance TADF Emitter

Janine Haug[1,2,3], André Jung[3], Piotr Banachowicz[3], Olaf Fuhr[4], Stefan Bräse[1,2], Eli Zysman-Colman[3]

1. Institute of Organic Chemistry, Karlsruhe Institute of Technology (KIT
2. Institute of Biological and Chemical Systems - Functional Molecular Systems, Karlsruhe Institute of Technology (KIT
3. Organic Semiconductor Centre, EaStCHEM School of Chemistry, University of St Andrews
4. Institute of Nanotechnology (INT) and Karlsruhe Nano-Micro Facility (KNMFi, Karlsruhe Institute of Technology (KIT

Abstract

Red-shifting MR-TADF emitters via donor substitution is an established strategy; however, this typically results in broadened emission and reduced photoluminescence quantum yields (FPL). We report tBuInPZ-DiKTa, fusing an indolophenazine donor directly to the DiKTa core, achieving an unprecedented red-shift for fused DiKTa-based emitters while preserving narrowband emission and high FPL.

Posted on 7 September 2026 — CC-BY 4.0 — This is a preprint and has not been peer reviewed. Data may be preliminary. — https://doi.org/10.26434/chemrxiv.15008386/v1

Molecular Engineering of a Small-Molecular Yellow-to-Orange Carbonyl-based Multi-Resonance TADF Emitter

Janine Haug[+a,b,c], André Jung[+c], Piotr Banachowicz[c], Olaf Fuhr[d], Stefan Bräse[a,b], Eli Zysman-Colman*[c]*

[+] These authors contributed equally

[a] Institute of Biological and Chemical Systems - Functional Molecular Systems, Karlsruhe Institute of Technology (KIT), Hermann-von-Helmholtz-Platz 1, 76344 Eggenstein-Leopoldshafen, Germany. E-mail: braese@kit.edu

[b] Institute of Organic Chemistry, Karlsruhe Institute of Technology (KIT), Kaiserstrasse 12, 76131 Karlsruhe, Germany. E-mail: braese@kit.edu

[c] Organic Semiconductor Centre, EaStCHEM School of Chemistry, University of St Andrews, St Andrews KY16 9ST, Fife, UK. E-mail: eli.zysman-colman@st-andrews.ac.uk

[d] Institute of Nanotechnology (INT) and Karlsruhe Nano-Micro Facility (KNMFi), Karlsruhe Institute of Technology (KIT), Kaiserstrasse 12, 76131 Karlsruhe, Germany.

Abstract

Red-shifting MR-TADF emitters via donor substitution is an established strategy; however, this typically results in broadened emission and reduced photoluminescence quantum yields (Φ_{PL}). We report **tBuInPZ-DiKTa**, fusing an indolophenazine donor directly to the **DiKTa** core, achieving an unprecedented red-shift for fused **DiKTa**-based emitters while preserving narrowband emission and high Φ_{PL}.

Introduction

Thermally activated delayed fluorescence (TADF) is a dual-emission photophysical process whereby a fast prompt fluorescence results from rapid depopulation of the S_1 excited state and a delayed emission is observed from the same S_1 following intersystem crossing (ISC) and reverse ISC (RISC) cycling.[1] One class of TADF emitters is multiresonant TADF (MR-TADF), polycyclic aromatic hydrocarbons containing judiciously positioned p- and n-dopants. This pattern of dopants produces excited states of short-range charge transfer (SRCT) character and singlet-triplet energy gaps (ΔE_{ST}) that are typically on the order of 150 meV.[1, 2] There are two main families of MR-TADF emitters based on the choice of n-dopant, either boron atoms or ketone groups.[3] The first example of a ketone-based MR-TADF emitter is the compound **QAO** (aka **DiKTa**), which has a central nitrogen atom and two ketone groups (**Fig. 1**).[4] **DiKTa** emits at a λ_{PL} of 460 nm, has a full-width at half maximum (FWHM) of 33 nm (193 meV) in toluene, and has a moderately large ΔE_{ST} of 0.20 eV.[5] One strategy to red-shift the emission of this family of MR-TADF compounds is to decorate the MR-TADF core with electron-donating groups, exemplified by **Cz-DiKTa** (**Fig. 1**). A second strategy is to embed another p-dopant. This is particularly attractive for organic light-emitting diode applications as the small molecular size and weight are preserved, enabling vacuum deposited devices to be fabricated; further, the rigid structure reduces geometry relaxation in the excited state, producing narrowband emission.[6, 7] Zou *et al.* reported the emitters **OQAO** and **SQAO** (**Fig. 1**), incorporating the electron-donating oxygen and sulfur chalcogens as bridging atoms, respectively.[5] The photoluminescence (PL) spectra of **OQAO** and **SQAO** in toluene are red-shifted compared to **DiKTa** to λ_{PL} of 520 and 552 nm, respectively, and have FWHM of 162 and 216 meV (36 and 54 nm), respectively. The broader emission of **SQAO** is attributed to the increased CT character of the emissive excited state due to the phenothiazine moiety.[8] There is no appreciable change in the ΔE_{ST}, being 0.16 eV for both.

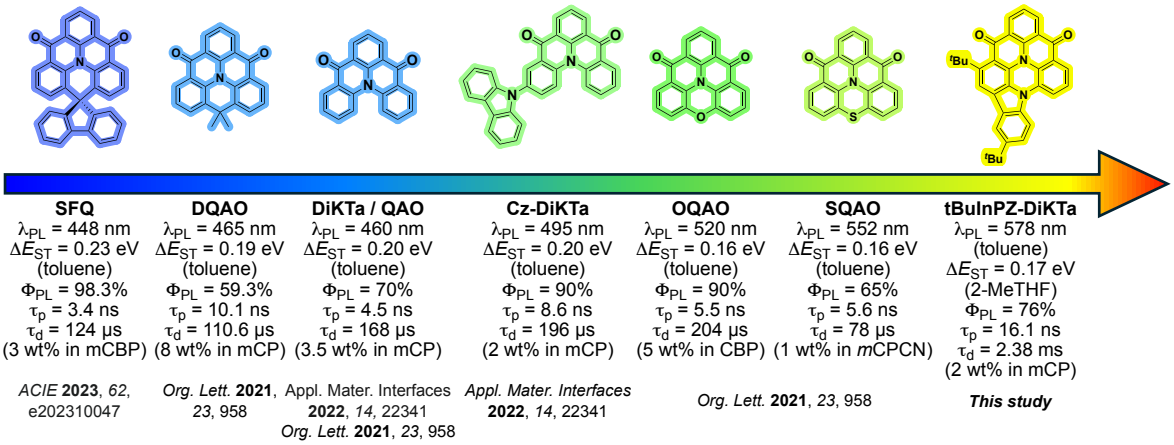


Fig. 1 (a) Selected structurally related **DiKTa**-based emitters with their photophysical properties, sorted by their λ_{PL} in dilute toluene solution.

Results and Discussion

With the objective to shift the emission of carbonyl-based MR-TADF emitters towards the red, while retaining a small molecular weight, we screened the HOMO levels of a series of *N*-heterocyclic donors at the PBE0/6-31G(d,p) level in the gas phase (**Fig. S26**). **InPZ** has the shallowest HOMO energy among the donor units screened (-4.74 eV), which is ca. 1 eV destabilized compared to carbazole (**Cz**) (HOMO of -5.73 eV), and more destabilized than that of **PXZ** (HOMO of −4.92 eV) and **PTZ** (HOMO of −4.89 eV). The PL of the corresponding reported fused **DiKTa**-based derivatives **OQAO** and **SQAO** (λ_{PL} of 520 and 552 nm in toluene) is significantly red-shifted compared to **DiKTa** (λ_{PL} of 460 nm in toluene).[5] Based on these calculations, the emitter **tBuInPZ-DiKTa** was designed, integrating *tert*-butyl groups to mitigate aggregation-caused quenching and improve solubility. The synthesis of **tBuInPZ-DiKTa** is shown in **Fig. 2**. Nucleophilic aromatic substitution of 1-fluoro-2-nitrobenzene (**2**) with 3,6-di-*tert*-butyl-9*H*-carbazole (**1**) yielded intermediate **3** in 99% yield. The subsequent Cadogen reaction afforded the **tBuInPZ** donor **4** in 56% yield, which was then subjected to nucleophilic aromatic substitution conditions with 2-fluoroisophthalonitrile (**5**), affording intermediate **6** in 56% yield. The last step comprised hydrolysis of the nitrile groups, followed by activation of the acid with oxalyl chloride and then a Friedel-Crafts-type ring closing reaction catalyzed by $SnCl_4$, producing **tBuInPZ-DiKTa** in 21% yield. An attempt to access the corresponding phenylphenazine-fused DiKTa derivative through an analogous Friedel–Crafts-type cyclization was unsuccessful, instead resulting in the formation of persistent phenazine radical species (**Fig. S1**).

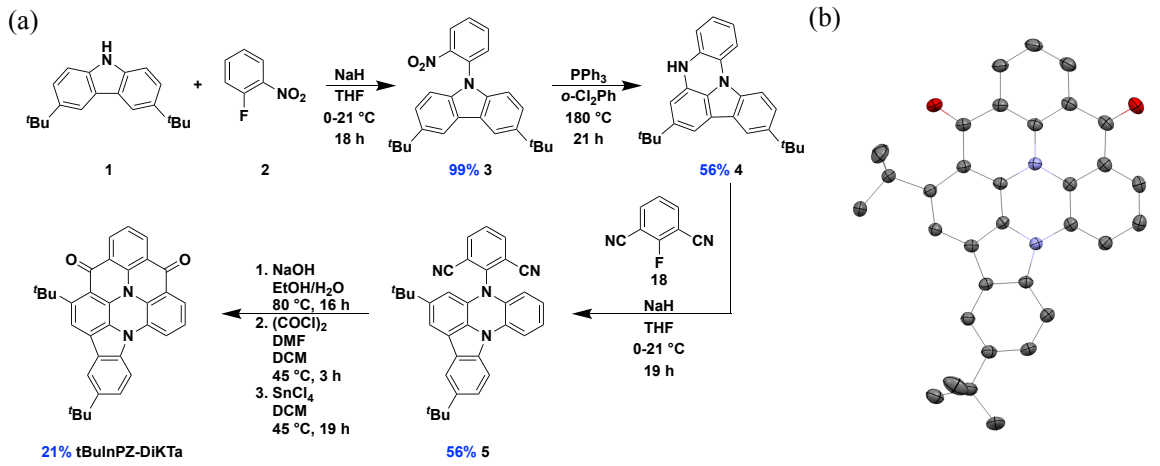


Fig. 2 (a) Synthetic route towards **tBuInPZ-DiKTa**. (b) Molecular structure of **tBuInPZ-DiKTa** (displacement parameters are drawn at 50% probability level). Hydrogen atoms and solvent molecules have been omitted for clarity.

The molecular structure of **tBuInPZ-DiKTa** was confirmed by single crystal X-ray diffraction measurements (CCDC-2580876, **Fig. S24**). The structure of **tBuInPZ-DiKTa** is much more planar than **DiKTa** (CCDC-1935488) (**Fig. S25**). The compound crystallizes in the triclinic space group P-1. The molecules stack on top of one another in columns related by the crystallographic inversion center, with the emitter orientation evident from the *tert*-butyl groups alternating between successive layers. Along the stack, the central nitrogen atoms show alternating short and long N···N distances of 3.588 and 5.643 Å.

The frontier molecular orbitals (FMOs) of **tBuInPZ-DiKTa** were modelled at the PBE0/6-31G(d,p) level of theory and the excited-state energies and electron density distributions were calculated at the RI-SCS-ADC(2)/cc-pVDZ level of theory as this includes double excitations, allowing for a more accurate modelling.[9] The calculated values are summarized in **Table S2** and the electron density plots are shown in **Fig. S27**. The HOMO energy of **tBuInPZ-DiKTa** is -5.50 eV, which is destabilized compared to those of **DiKTa** (E_{HOMO} = -6.20 eV), **OQAO** (E_{HOMO} = -5.87 eV), and **SQAO** (E_{HOMO} = -5.88 eV). The electron density plot reveals that the HOMO is delocalized across the entire p-system of **tBuInPZ-DiKTa**. For **OQAO** and **SQAO**, the HOMO extends onto the bridging oxygen or sulfur atom, respectively. The LUMO levels for **DiKTa**, **OQAO**, **SQAO**, and **tBuInPZ-DiKTa** are, however, comparable, ranging between -2.23 and -2.35 eV, reflecting a similar electron density distribution and a large decoupling of the electron densities of these orbitals. The resulting HOMO-LUMO gap, ΔE, of 3.19 eV for **tBuInPZ-DiKTa** is narrowed compared to **DiKTa** (3.97 eV), **OQAO** (3.55 eV), and **SQAO** (3.53 eV). Similar electron density patterns are evident for the S_1 and T_1 states across these emitters, extending over the entire fused donor fragments for **OQAO**, **SQAO**, and **tBuInPZ-DiKTa**. The energies of the S_1 and T_1 states are significantly stabilized to 2.61 and 2.37 eV for **tBuInPZ-DiKTa** compared to 3.28 eV and 3.01 for **DiKTa** as well as for **OQAO** (S_1 of 2.91

eV, T_1 of 2.69 eV) and **SQAO** (S_1 of 2.99 eV, T_1 of 2.81 eV). This results in ΔE_{ST} of 0.27, 0.22, 0.18, and 0.24 eV for **DiKTa**, **OQAO**, **SQAO**, and **tBuInPZ-DiKTa**, respectively, indicating that RISC should be operational in **tBuInPZ-DiKTa** to enable TADF. The T_2 state of **DiKTa** is of similar energy to the S_1 state (3.28 eV), facilitating ISC and RISC, while the T_2 states of **OQAO**, **SQAO**, and **tBuInPZ-DiKTa** (3.45, 3.31, and 3.02 eV) are at much higher energy than their corresponding S_1 states (2.91, 2.99, and 2.61 eV). The spin-orbit coupling between T_1 and S_1 is weakened for all emitters compared to **DiKTa** ($\langle S_1|H_{SO}|T_1\rangle$ of 1.84 cm^{-1}), with low $\langle S_1|H_{SO}|T_1\rangle$ values in the range of 0.00–0.07 cm^{-1}. Similar oscillator strengths (*f*) for the S_0-S_1 transition in the range of 0.16–0.23 are predicted for all emitters. To gain deeper insight into the excited-state CT character and vibronic coupling of these emitters, we calculated the Δr_{S1} descriptor, representing the hole-electron distances,[10] the Huang Rhys factors (HRf) and the corresponding mode-resolved reorganization energies (**Fig. S28**).[11-13] **DiKTa** has the smallest Δr_{S1} value of 1.138 Å followed by **OQAO** (1.848 Å), **tBuInPZ-DiKTa** (2.377 Å), and **SQAO** (2.511 Å). The larger Δr_{S1} of **SQAO** compared to **tBuInPZ-DiKTa** indicates a more pronounced CT character in **SQAO**. Introduction of the bridging atoms in **tBulnPZ-DiKTa**, **OQAO**, and **SQAO** effectively suppresses low-frequency vibrational mode contributions (<250 cm^{-1}) to the reorganization energy compared with the parent **DiKTa**. For **tBuInPZ-DiKTa**, the maximum HRf (HRf_{max}) is 0.2 in the low-to-mid-frequency region (250-1250 cm^{-1}) and remains below 0.1 at higher frequencies (1250-2000 cm^{-1}), which indicates minimal displacements between the ground and excited states, while in **DiKTa** the HRf_{max} are 1.1 and 0.14 in these regions, respectively. The total reorganization energy (λ_{ROE}) of **tBulnPZ-DiKTa** (127 meV) is lower compared to **DiKTa** (144 meV), **OQAO** (151 meV) and **SQAO** (164 meV), which, together with Δr_{S1}, reflects the trend in FWHM of the emission bands.

Cyclic and differential pulse voltammograms (CV and DPV, respectively) were recorded in degassed dichloromethane (DCM) solution (**Fig. S29**, **Table S3**). The CV of **tBuInPZ-DiKTa** shows reversible oxidation and reduction waves, with an oxidation potential (E_{ox}) of 1.05 V and reduction potential (E_{red}) of -1.29 V, both obtained from the corresponding DPV. The E_{ox} of **tBuInPZ-DiKTa** (1.05 V) is cathodically shifted compared to those of **DiKTa**[14] (E_{ox} of 1.78 V), **OQAO**[5] (E_{ox} of 1.50 V), and **SQAO**[5] (E_{ox} of 1.31 V), while each of these compounds has a similar E_{red} (-1.25 to -1.35 V). This behavior is consistent with the DFT picture. The redox potentials translate to HOMO and LUMO energies of -5.39 and -3.05 eV, respectively, for **tBuInPZ-DiKTa**. The resulting electrochemical gaps, DE_{redox}, decrease progressively with increasing donor strength from 3.10 eV for **DiKTa**,[14] to 2.77 eV for **OQAO**,[5] 2.56 eV for **SQAO**,[5] and 2.34 eV for **tBuInPZ-DiKTa**.

The photophysical properties of **tBuInPZ-DiKTa** in dilute toluene are summarized in **Table 1** and the spectra are shown in **Fig. 3**. The absorption and emission spectra show the expected mirror image profile of rigid fluorophores (**Fig. 3a**). The absorption spectrum shows two overlapping low-energy absorption

bands with λ_{abs} for the SRCT at 542 nm (ε of 9.5 × 10^3 M^{-1} cm^{-1}) and the other band of slightly higher energy at λ_{abs} of 510 nm (ε of 6.1 × 10^3 M^{-1} cm^{-1}). This SRCT band is red-shifted compared to both **OQAO**[5] and **SQAO**,[5] which both have SRCT bands at λ_{abs} of 489 nm (the ε was not reported). The emission of **tBuInPZ-DiKTa** peaks at λ_{PL} of 578 nm, significantly red-shifted compared to that of **DiKTa**[5] (λ_{PL} of 460 nm) and a more pronounced red-shift than observed for **OQAO**[5] and **SQAO**[5] with λ_{PL} of 520 and 552 nm, respectively. The PL spectrum of **tBuInPZ-DiKTa** is narrowband, characterized by its FWHM of 162 meV (43 nm). While the spectral profile is similar to that of **OQAO**[5] (FWHM of 162 meV, 36 nm), it is narrowed compared to **DiKTa**[5] (FWHM of 193 meV, 33 nm) and **SQAO**[5] (FWHM of 216 meV, 54 nm), likely due to the interplay between the predicted CT character of **tBuInPZ-DiKTa** and the suppression of low-frequency vibrational modes. While the calculated λ_{ROE} of **tBuInPZ-DiKTa** (127 meV) is the lowest of the series, its relatively large Δr_{S1} (2.377 Å) is responsible for the relatively broader emission compared to that of **OQAO**, which has a λ_{ROE} (151 meV). The PL solvatochromism study reveals that the emission red-shifts in solvents of increasing polarity, coupled with a broadening of the spectrum and a loss of the vibrational structure (**Fig. 3b**). This behavior is consistent with an increased admixture of long-range CT character to the emissive state.

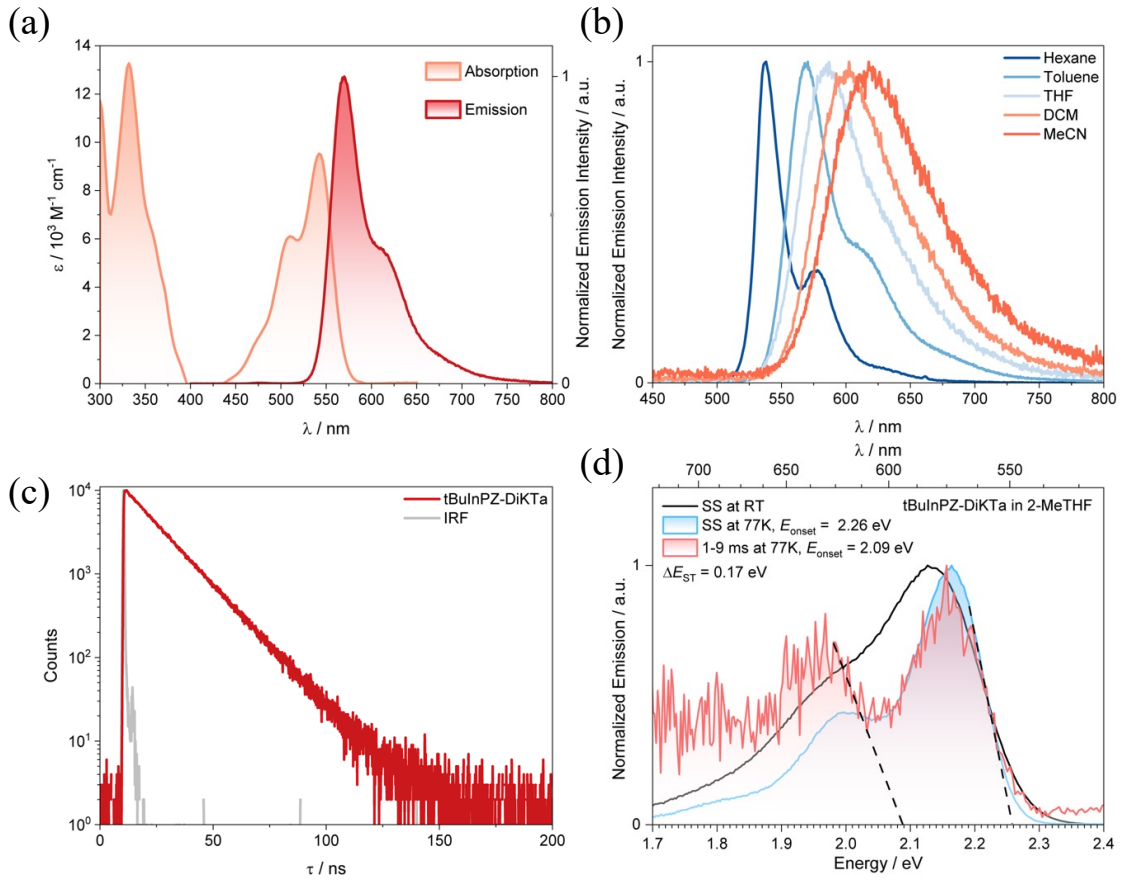


Fig. 3 (a) Absorption and PL spectra in toluene solution (λ_{exc} = 328 nm). (b) PL solvatochromism study (λ_{exc} = 351 nm). (c) Time-resolved PL decay in toluene solution (TCSPC, c = 10^{-5} M, λ_{exc} = 375 nm). (d) Steady-state PL (77K, RT) and delayed emission spectra (1-10 ms, 77 K) in 2-MeTHF (λ_{exc} = 375 nm).

The time-resolved PL measurement shows monoexponential decay kinetics, with a prompt lifetime τ_p of 14.8 ns (**Fig. 3c**). This is longer than that of **DiKTa** at 5.1 ns.[15] **tBuInPZ-DiKTa** has a high Φ_{PL} of 88% in degassed toluene, which decreases to 79% upon exposure to air. This is significantly increased compared to **DiKTa**[15] (Φ_{PL} of 26% in degassed toluene); the values of **OQAO** and **SQAO** were not reported. The ΔE_{ST} was determined from the onsets of the steady-state PL and delayed emission spectra at 77 K in 2-MeTHF glass (**Fig. 3d**). The energies of the S_1 and T_1 states, E_{S1} and E_{T1}, of 2.26 and 2.09 eV, respectively, are stabilized compared to those of **DiKTa**[5] (E_{S1} of 2.69 eV, E_{T1} of 2.49 eV in solid toluene), similar to **SQAO**[5] (E_{S1} of 2.23 eV, E_{T1} of 2.07 eV in solid toluene) and slightly stabilized compared to **OQAO**[5] (E_{S1} of 2.34 eV, E_{T1} of 2.18 eV, in solid toluene). The resulting ΔE_{ST} of **tBuInPZ-DiKTa** is similar to those of **DiKTa**,[5] **OQAO**,[5] and **SQAO**,[5] all ranging between 0.16 and 0.20 eV, typical for MR-TADF compounds.[2, 3]

Subsequently, the photophysical properties of spin-coated doped films of **tBuInPZ-DiKTa** in 1,3-bis(*N*-carbazolyl)benzene (mCP), a high triplet energy host (E_T = 2.90 eV), were determined (**Table 1**, **Fig. 4**).[16] The PL spectrum of the 2 wt% doped film is broader and red-shifted than that in solution, peaking at λ_{PL} of 587 nm and having a FWHM of 206 meV (59 nm) (**Fig. 4a**). The emission of the doped films of **tBuInPZ-DiKTa** is red-shifted compared to those of **DiKTa**[17] (λ_{PL} of 466 nm, 2 wt% doped in mCP), **OQAO**[5] (λ_{PL} of 534 nm, 5 wt% doped in CBP), and **SQAO**[5] (λ_{PL} of 560 nm, 1 wt% doped in mCPCN). The PL of **tBuInPZ-DiKTa** is narrower than those of **DiKTa**[17] and **SQAO**,[5] with FWHM of 222 and 233 meV (40 and 60 nm), respectively, and is slightly broadened compared to the FWHM of **OQAO**[5] of 192 meV (45 nm). The PL spectrum of **tBuInPZ-DiKTa** shifts slightly to the red, without significant broadening across doping concentrations ranging between 1 and 5 wt%. The Φ_{PL} of the 1, 2, and 5 wt% doped films are 74, 76, and 66%, which decrease in air to 60, 56, and 56%, respectively. The Φ_{PL} of **tBuInPZ-DiKTa** is slightly higher than those of **DiKTa**[17] and **SQAO** (70 and 65%, respectively), while **OQAO**[5] has the highest reported Φ_{PL} of 90%.

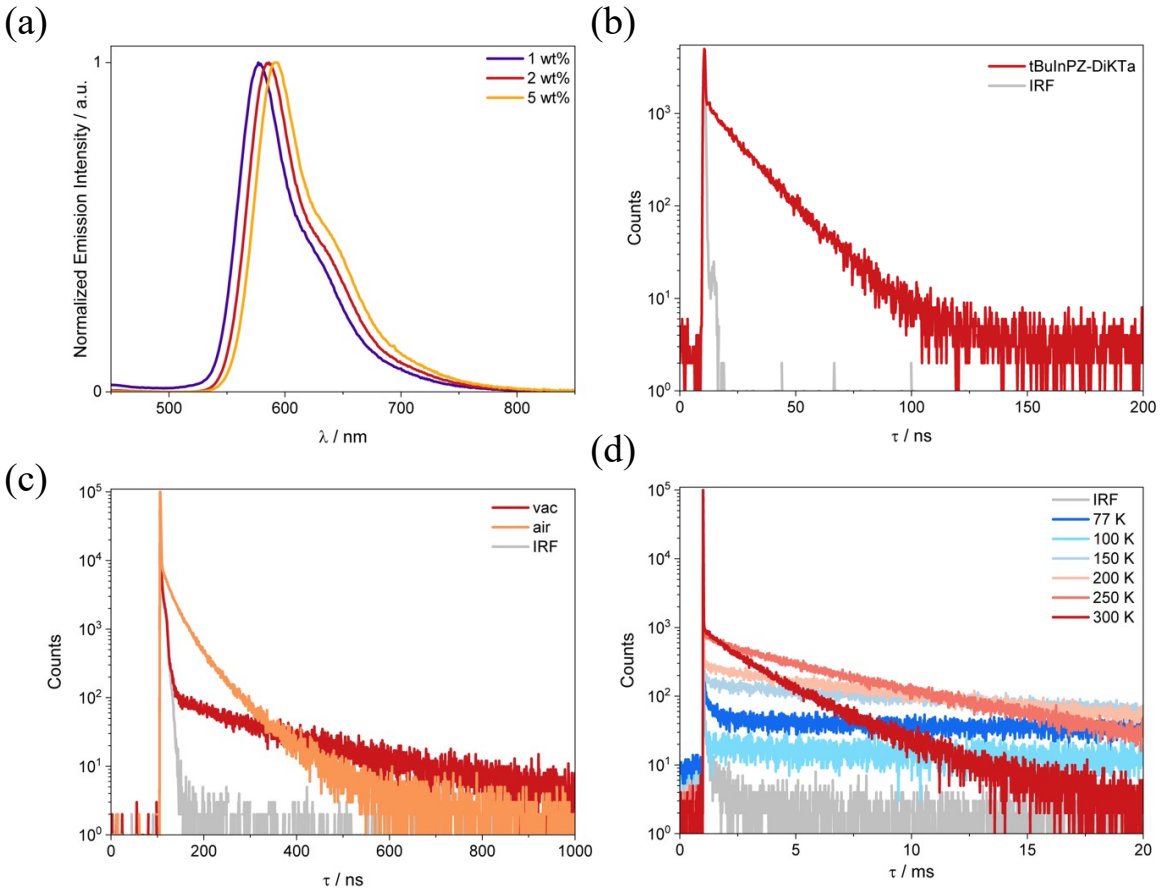


Fig. 4 (a) PL spectra of 1, 2, and 5 wt% doped films in mCP (λ_{exc} = 341 nm). (b) Time-resolved PL decay of the 2 wt% doped mCP film (MCS, λ_{exc} = 341 nm) in vacuo and air. Inset: time-resolved PL decay of the 2 wt% doped mCP film (TCSPC, λ_{exc} = 375 nm). (c) Temperature-dependent time-resolved PL decay of the 2 wt% doped film in mCP (MCS, λ_{exc} = 341 nm). (d) Steady-state PL (77K and RT) and delayed emission spectra (77 K) 2 wt% doped mCP film (λ_{exc} = 341 nm).

The PL of the 2 wt% doped films of **tBuInPZ-DiKTa** in mCP decays with multiexponential kinetics (**Fig. 4b**). Using TCSPC, the prompt PL decays with monoexponential kinetics, with a τ_p of 16.1 ns, while using MCS, the delayed emission decays with biexponential kinetics, with a $\tau_{d,avg}$ of 2.38 ms. The τ_p is longer compared to that of **DiKTa**[17] (2 wt% doped in mCP), **OQAO**[5] (5 wt% in CBP), and **SQAO**[5] (1 wt% in mCPCN) with values of 4.5, 5.5, and 5.6 ns, respectively. Similarly, the $\tau_{d,avg}$ is significantly longer than the reported 168 µs for **DiKTa**,[17] 204 µs for **OQAO**,[5] and the 78 µs for **SQAO**.[5] In air, the τ_p of **tBuInPZ-DiKTa** is 15.1 ns and $\tau_{d,avg}$ is 377 µs. An additional decay with a lifetime of 202 ns is present in air, which potentially reflects the environmental heterogeneity within the film. In oxygen-accessible surface and porous regions, efficient triplet quenching significantly shortens the triplet lifetime and produces the short-lived component with a low intensity, while in dense, shielded regions the triplets are protected from oxygen and up-convert on a much longer timescale, giving rise to the long delayed lifetime. The ΔE_{ST} of the 2 wt% doped films in mCP was determined to be 0.04 eV (**Fig. 4d**), which is a lot smaller than expected from the calculations, the ΔE_{ST} determined in solution,

and the TRPL measurements (***Error! Reference source not found.*d**). This likely reflects the impact of the environmental effects of the host matrix on the relative energies of the excited singlet and triplet states. Temperature-dependent TRPL measurements showed that the delayed emission intensity increases with increasing temperature, reflective of TADF (**Fig. 4c**).

The excitonic kinetics were estimated, following the methodology reported by Tsuchiya *et al.*[18] and compared to the literature values inferred from the photophysical data for the 2 wt% doped films of **DiKTa** in mCP (Table **S4**). The ISC and RISC rate constants of **tBuInPZ-DiKTa** are 4.22×10^7 s^{-1} and 8.11×10^2 s^{-1}, respectively, slower than those of **DiKTa** of 19.4×10^7 s^{-1} and 2.48×10^4 s^{-1}, respectively.

Table 1 Summary of photophysical data

Emitter	Medium	λ_{Abs} / nm	λ_{PL} / nm	FWHM / nm (meV)	Φ_{PL} (air) / %	τ_p /ns	τ_d /µs	E_{S1} / eV	E_{T1} / eV	ΔE_{ST} / eV
DiKTa	Sol.[5, 15]	433[a]	460[a]	33 (193)[a]	26[a]	5.1	23	2.69[j]	2.49[j]	0.20[j]
	Film[b 17]	N/A	466	40 (222)	70	4.5	168	2.75	2.55	0.20
tBuInPZ-DiKTa	Sol.	542[a]	578[a]	43 (162)[a]	88 (79)[f]	14.8[h]	-	2.26[k]	2.09 [k]	0.17[k]
	Film[b]	N/A	587[e]	59 (206)[e]	76 (56)[g]	16.1[i]	2380[i]	2.27[l]	2.23[l]	0.04[l]
OQAO[5]	Sol.	489[a]	520[a]	36 (162)[a]	N/A	N/A	N/A	2.34[j]	2.18[j]	0.16[j]
	Film[c]	N/A	534	45 (192)	90	5.5	204	N/A	N/A	N/A
SQAO[5]	Sol.	489[a]	552[a]	54 (216)[a]	N/A	N/A	N/A	2.23[j]	2.07[j]	0.16[j]
	Film[d]	N/A	560	60 (233)	65	5.6	78	N/A	N/A	N/A

[a] In dilute toluene solution (c = 10^{-5} M, **tBuInPZ-DiKTa**: λ_{exc} = 328 nm). [b] 2 wt% in mCP. [c] 5 wt% in CBP. [d] 1 wt% in mCPCN. [e] λ_{exc} = 341 nm. [f] Relative method in degassed (aerated) toluene with Rhodamine 6G[19] (Φ_{PL} = 95%, 10^{-5} M in EtOH; λ_{exc} = 530 nm). [g] Absolute method using an integrating sphere in N_2 (air) (λ_{exc} = 341 nm). [h] In degassed toluene (TCSPC, c = 10^{-5} M, λ_{exc} = 375 nm). [i] In film under N_2 (air) (prompt: TCSPC, λ_{exc} = 375 nm; delayed: MCS, λ_{exc} = 341 nm). [j] In toluene solution. [k,l] From the onsets of the SS-PL and delayed emission spectra at 77 K in [k] 2-MeTHF (λ_{exc} = 375 nm) and [l] doped film (λ_{exc} = 341 nm).

Summary

We have designed and characterized the MR-TADF emitter **tBuInPZ-DiKTa**, fusing the strong indolophenazine donor **tBuInPZ** within the **DiKTa** framework. The PL of **tBuInPZ-DiKTa** is significantly red-shifted compared to the parent **DiKTa** at λ_{PL} of 578 nm (in toluene) and 587 nm (2 wt% mCP films), while its spectrum remains narrowband (FWHM of 43 nm or 162 meV in toluene and 59 nm or 206 meV in 2 wt% mCP film). The compound has a high Φ_{PL} of 76% (56% in air), a τ_p of 16.1 ns and a τ_d of 2.38 ms in 2 wt% doped films in mCP. The ΔE_{ST} is 0.17 eV in 2-MeTHF glass at 77 K. These findings demonstrate that fusing a strong indolophenazine donor like **tBuInPZ** into **DiKTa** provides a viable strategy toward a small-molecular weight MR-TADF compound showing bright, narrowband and strongly red-shifted emission.

Conflicts of interest

There are no conflicts to declare.

Supporting Information

^{1}H NMR and ^{13}C NMR spectra, HRMS, IR, HPLC; supplementary computational data and coordinates; crystallographic data, additional photophysical data.

Acknowledgments

J.H. gratefully acknowledges funding from the Studienstiftung des deutschen Volkes. We thank the EPSRC (EP/Z535291/1 and EP/W007517/1) for financial support. The authors acknowledge support by the state of Baden-Württemberg through bwHPC and the German Research Foundation (DFG) through grant no INST 40/575-1 FUGG (JUSTUS 2 cluster).

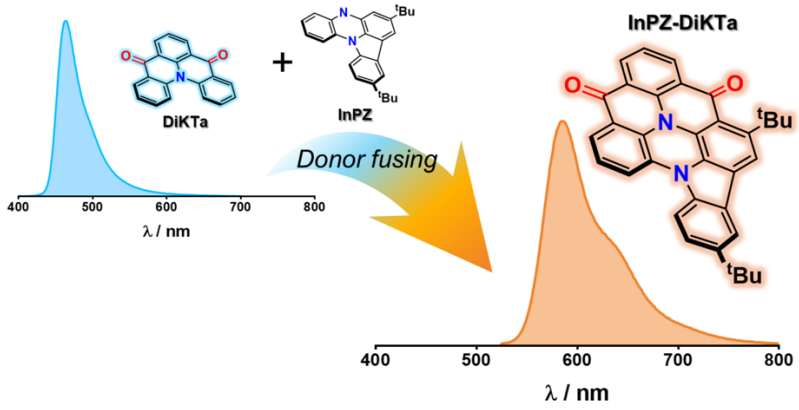
Data Availability Statement

The research data supporting this publication can be accessed at https://dx.doi.org/10.14272/collection/AJ_2024-09-23.

Author Contributions

CRediT: J.H.: conceptualization, data curation, formal analysis, investigation, methodology, visualization, writing - original draft, writing - review & editing. A.J.: conceptualization, data curation, formal analysis, investigation, methodology, visualization, writing - original draft, writing - review & editing. P.B.: data curation, formal analysis, investigation, writing - review & editing. O.F.: formal analysis, investigation, writing - review & editing. S.B.: conceptualization, funding acquisition, methodology, project administration, resources, supervision, writing - review & editing. E.Z.-C.: conceptualization, funding acquisition, methodology, project administration, resources, supervision, writing - review & editing.

TOC Graphic



References

1. J. M. Dos Santos, D. Hall, B. Basumatary, M. Bryden, D. Chen, P. Choudhary, T. Comerford, E. Crovini, A. Danos, J. De, S. Diesing, M. Fatahi, M. Griffin, A. K. Gupta, H. Hafeez, L. Hämmerling, E. Hanover, J. Haug, T. Heil, D. Karthik, S. Kumar, O. Lee, H. Li, F. Lucas, C. F. R. Mackenzie, A. Mariko, T. Matulaitis, F. Millward, Y. Olivier, Q. Qi, I. D. W. Samuel, N. Sharma, C. Si, L. Spierling, P. Sudhakar, D. Sun, E. Tankelevičiūtė, M. Duarte Tonet, J. Wang, T. Wang, S. Wu, Y. Xu, L. Zhang and E. Zysman-Colman, *Chem. Rev.*, 2024, **124**, 13736-14110.
2. S. Madayanad Suresh, D. Hall, D. Beljonne, Y. Olivier and E. Zysman-Colman, *Adv. Funct. Mater.*, 2020, **30**, 1908677.
3. X. Wu, S. Ni, C.-H. Wang, W. Zhu and P.-T. Chou, *Chem. Rev.*, 2025, **125**, 6685-6752.
4. Y. Yuan, X. Tang, X. Y. Du, Y. Hu, Y. J. Yu, Z. Q. Jiang, L. S. Liao and S. T. Lee, *Adv. Optical Mater.*, 2019, **7**, 1801536.
5. S.-N. Zou, C.-C. Peng, S.-Y. Yang, Y.-K. Qu, Y.-J. Yu, X. Chen, Z.-Q. Jiang and L.-S. Liao, *Org. Lett.*, 2021, **23**, 958-962.
6. C. Shen, Y. Hu, S. Zhou, Z. He, J. Han, D. Zhang, L. Lu, X. Mo and Q. Zhang, *Adv. Electron. Mater.*, 2025, **11**, e00555.
7. K. R. J. Thomas, V. Rajendran and C.-H. Chen, *ChemPhotoChem*, 2025, **9**, e202500276.
8. A. T. Gogoulis, R. Hojo, K. Bergmann and Z. M. Hudson, *Org. Lett.*, 2023, **25**, 7791-7795.
9. D. Hall, J. C. Sancho-García, A. Pershin, G. Ricci, D. Beljonne, E. Zysman-Colman and Y. Olivier, *J. Chem. Theory Comput.*, 2022, **18**, 4903-4918.
10. C. A. Guido, P. Cortona, B. Mennucci and C. Adamo, *J. Chem. Theory Comput.*, 2013, **9**, 3118-3126.
11. Z. Shuai and Q. Peng, *Phys. Rep.*, 2014, **537**, 123-156.
12. Z. Shuai and Q. Peng, *Natl. Sci. Rev.*, 2017, **4**, 224-239.
13. Z. Shuai, *Chin. J. Chem.*, 2020, **38**, 1223-1232.
14. S. Wu, W. Li, K. Yoshida, D. Hall, S. Madayanad Suresh, T. Sayner, J. Gong, D. Beljonne, Y. Olivier, I. D. W. Samuel and E. Zysman-Colman, *ACS Appl. Mater. Interfaces*, 2022, **14**, 22341-22352.
15. D. Hall, S. M. Suresh, P. L. dos Santos, E. Duda, S. Bagnich, A. Pershin, P. Rajamalli, D. B. Cordes, A. M. Z. Slawin and D. Beljonne, *Adv. Optical Mater.*, 2020, **8**, 1901627.
16. C. Xiang, X. Fu, W. Wei, R. Liu, Y. Zhang, V. Balema, B. Nelson and F. So, *Adv. Funct. Mater.*, 2016, **26**, 1463-1469.
17. S. Wu, A. Kumar Gupta, K. Yoshida, J. Gong, D. Hall, D. B. Cordes, A. M. Z. Slawin, I. D. W. Samuel and E. Zysman-Colman, *Angew. Chem. Int. Ed.*, 2022, **61**, e202213697.
18. Y. Tsuchiya, S. Diesing, F. Bencheikh, Y. Wada, P. L. dos Santos, H. Kaji, E. Zysman-Colman, I. D. W. Samuel and C. Adachi, *J. Phys. Chem. A*, 2021, **125**, 8074-8089.
19. D. Magde, R. Wong and P. G. Seybold, *Photochem. Photobiol.*, 2002, **75**, 327-334.